On ethanol droplet evaporation in the presence of background fuel vapor

Abgail P. Pinheiro[*1], João Marcelo Vedovoto[1], Aristeu da Silveira Neto[1], Berend G. M. van Wachem[2]

[1]School of Mechanical Engineering, Federal University of Uberlândia, Av. João Naves de Ávila, 2121, Bloco 5P, Uberlândia, Minas Gerais 38400-902, Brazil
[2]Chair of Mechanical Process Engineering, Otto-von-Guericke-Universität Magdeburg, Universitätsplatz 2, 39106 Magdeburg, Germany
*Corresponding author: abgail.pinheiro@gmail.com

Abstract
Ethanol is considered a promising alternative fuel due to its advantages when compared to conventional fossil fuels mostly because it is renewable, biodegradable, it has high octane number and latent heat of evaporation. Since droplets generally evaporate inside a vapor cloud in spray combustion, rather than burning individually, in a realistic setup, considering background fuel vapor concentration effects is crucial. Therefore, this work aims to investigate the effects of ambient fuel vapor concentration on the evaporation of a single ethanol droplet by means of numerical simulations to better understand its evaporation dynamics. The theoretical model is validated through numerical simulations of an ethanol droplet evaporation. The results show that condensation effects are observed for non-zero ambient vapor concentration at the beginning of the simulation. For low ambient temperature and high ambient pressure conditions, if the ambient fuel vapor concentration is high enough, the droplet does not evaporate. In this study, the ambient fuel vapor concentration is varied in the range of 0.0 to 0.75. The influence of ambient vapor concentration on the average area reduction rate is also investigated. Such influence is explained by the net result of mass and energy transfers factors. It is noticed that there is a threshold ambient temperature which determines whether the average area reduction rate will increase or decrease as function of the ambient vapor concentration.

Keywords
Droplet evaporation, Condensation, Numerical simulation, Ethanol

Introduction
In 2012, fossil fuels accounted for 84 % of the worldwide energy consumption. In 2040, even with the increase in renewable and nuclear energy, predictions have shown that fossil fuels will still account for 78 % of energy use [1]. As a consequence, the majority of the work that has studied effects of ambient pressure and temperature on droplet evaporation focused on fossil fuel components evaporation [12, 6, 9, 10]. However, as stated by Bergthorson and Thomson [5], there is a huge concern over greenhouse-gas emissions and petroleum scarcity that motivates the search for alternative fuels. In this context, ethanol provides a clean, efficient, and affordable energy source solution.

Ethanol is considered a promising alternative fuel because it can be derived from biomass via established processes, as proven by the evolution from first to third-generation biofuels; it seems to be easy merging its production and use with the existing infrastructure; and it has advantages when compared with conventional fuels [5]. Compared with gasoline, to illustrate, ethanol has a significantly higher octane number and latent heat of evaporation, which improves thermal and volumetric efficiencies and, consequently, reduces the emissions of pollutants, such as carbon monoxide, exhaust hydrocarbons and fine particulates. Moreover, ethanol is renewable and biodegradable [4, 17, 14].

Since droplet evaporation in the presence of background fuel vapor may be also important for practical applications, especially for dense sprays, the ambient vapor concentration should also be taken into account for mimicking the interaction with other droplets that are also evaporating. Such aspects were previously studied by Abarham and Wichman [2], but they have only considered propane droplets evaporating under low temperature and atmospheric pressure conditions. An in-depth investigation of how ambient conditions impact the ethanol vaporability is necessary for the development of new technology for ethanol-fueled internal combustion engines, and it will result in more functional and economical devices.

A number of experimental and numerical research works have already investigated the effects of ambient conditions on droplet evaporation behavior. However, none of these works have been carried out considering the joint effects of high ambient temperature, pressure and fuel vapor concentration. Some works [12, 6, 9, 10] have analyzed the joint effects of ambient conditions for a wide range of temperature and pressure, but assuming isolated droplets. The paper which has considered background fuel vapor concentration effects [2], did not take into account high temperature and pressure conditions. Moreover, to the best of the authors' knowledge, so far no systematic research has been performed to study background fuel vapor concentration effects for ethanol droplets. Since droplets generally evaporate inside a vapor cloud in spray combustion, rather than burning individually, in a realistic setup considering background fuel vapor concentration effects is crucial.

Therefore, the purpose of this study is to investigate the effects of background fuel vapor concentration on ethanol droplet evaporation for a wide range of ambient conditions used in certain practical situations. First, the predictions of the evaporation model proposed by Abramzon and Sirignano [3] are validated by comparison to experimental measurements. Furthermore, the ambient vapor concentration is varied in the ranges of $0.0-0.75$ to investigate the effects of multiple droplets evaporation, while the ambient pressure and temperature are varied in the ranges of $0.1-2.0$ MPa and $400-1000$ K, respectively.

Evaporation model
Mass and thermal energy transfer processes are described by differential equations, which express the temporal changes of droplet size and temperature. The droplet mass variation throughout time is given by:

$$\frac{dm_d}{dt} = -\dot{m}_d,\tag{1}$$

where m_d is the droplet mass and $\dot{m}_d$ is the droplet mass evaporation rate that leads directly to droplet size reduction:

$$\frac{dD_d}{dt} = -\frac{2\dot{m}_d}{\pi \rho_l D_d{}^2},\tag{2}$$

where D_d is the droplet diameter, ρ stands for density and the subscript l refers to the liquid phase. The droplet temperature variation as a function of time is given by:

$$m_d c_{p_l}\frac{dT_d}{dt} = Q_S,\tag{3}$$

where c_p is the specific heat capacity and Q_S is the power transferred to promote the droplet thermal energy variation per unit of time, which is transferred as heat.
Based on a detailed analysis of different evaporation models [13], the Abramzon-Sirignano evaporation model (ASM) [3] is adopted to represent the mass and energy transfers between the liquid and gaseous phases. In this model, the instantaneous droplet evaporation rate is given as:

$$\dot{m}_d = \pi D_d D_{vm} \rho_m Sh^*{}_m ln\left(1 + B_M\right),\tag{4}$$

where D_v is the vapor diffusion coefficient, subscript m represents that the physical properties are evaluated at the gas-vapor mixture conditions in the film around the droplet determined by the $1/3$ averaging rule [11], Sh^* is the modified Sherwood number proposed by Abramzon and Sirignano [3], which for this study is 2.0, since both droplet and ambient gas are still, and B_M is the Spalding mass transfer number given by:

$$B_M = \frac{Y_{vs} - Y_{vg}}{1 - Y_{vs}},\tag{5}$$

where Y_{vs} and Y_{vg} are the vapor mass fractions at the droplet surface and in the ambient gas far away from the droplet, respectively.
The vapor mass fraction at the droplet surface may be calculated using Raoult's law, which states that the surface vapor molar fraction, χ_{vs}, is equal to the ratio between the saturated vapor pressure, p_{vs}, and the ambient pressure, p_g:

$$\chi_{vs} = \frac{p_{vs}}{p_g},\tag{6}$$

Therefore, once χ_{vs} is determined, Y_{vs} can be computed as:

$$Y_{vs} = \frac{\chi_{vs} W_v}{\chi_{vs} W_v + \chi_{gs} W_g},\tag{7}$$

where W is the molecular weight, and subscripts v and g refer to the fuel vapor and the ambient gas, respectively. Assuming that the temperature inside the droplet is uniform, the energy balance equation for the surrouding gas, coupled to Fourier's law for the convective energy transfer between gas and liquid as the surface boundary condition, yields the following expression for the sensible energy used to increase the liquid droplet temperature during the heat-up period:

$$Q_S = G\pi D_d Nu^*{}_m k_m \left(T_g - T_d\right) - L_v \dot{m}_d,\tag{8}$$

where k is the thermal conductivity and Nu^* is the modified Nusselt number, which is equal to 2.0 because the droplet Reynolds number is assumed zero. The correction factor for energy transfer reduction due to the vapor diffusing out is:

$$G = \frac{ln\left(1 + B_T\right)}{B_T},\tag{9}$$

where B_T is the Spalding thermal energy transfer number:

$$B_T = \left(1 + B_M\right)^{\varphi} - 1,\tag{10}$$

where:

$$\varphi = \left(\frac{c_{p_v}}{c_{p_g}}\right)\left(\frac{Sh^*}{Nu^*}\right)\frac{1}{Le_m}, \tag{11}$$

where Le is the Lewis number:

$$Le_m = \frac{k_m}{c_{p_m}D_{vm}\rho_m}. \tag{12}$$

ASM is implemented in the in-house code MFSim and it is used for the simulations in this work. The 4th-order Runge-Kutta scheme is used for the time discretization of Eqs. (2) and (3) to predict the temporal advancement of droplet size and temperature.

The physical properties for vapor and gas, identified with subscripts v and g, are obtained utilizing the open source Cantera software package [7], based on the phase molar composition and reference temperature at the gas-vapor mixture, T_m. Furthermore, the diffusivity of fuel vapor in gas, D_{vm}, even when the gaseous phase is a mixture, is also directly calculated by Cantera as a function of molar composition, reference temperature and ambient pressure. The liquid droplet properties, ρ_l and c_{p_l}, the latent heat of evaporation, and the saturated vapor pressure are calculated based on the database found in Green and Perry [8]. Finally, all the thermodynamic and transport properties for liquid, vapor and gas phases are assumed constant during each time step, but they vary from one time step to another due to the corresponding changes in droplet temperature.

Results and discussion
Model validation
The ASM predictions for anhydrous ethanol droplets are compared to the experimental measurements of Saharin *et al.* [18]. The experiments were performed in a furnace with nitrogen as the ambient gas to prevent oxidation or ignition. The fuel droplets, with an initial diameter between 430 and 609 μm, were supported in a cross-fiber system. In all experiments the ambient pressure is kept atmospheric, while the temperature varied from 473 to 673 K.
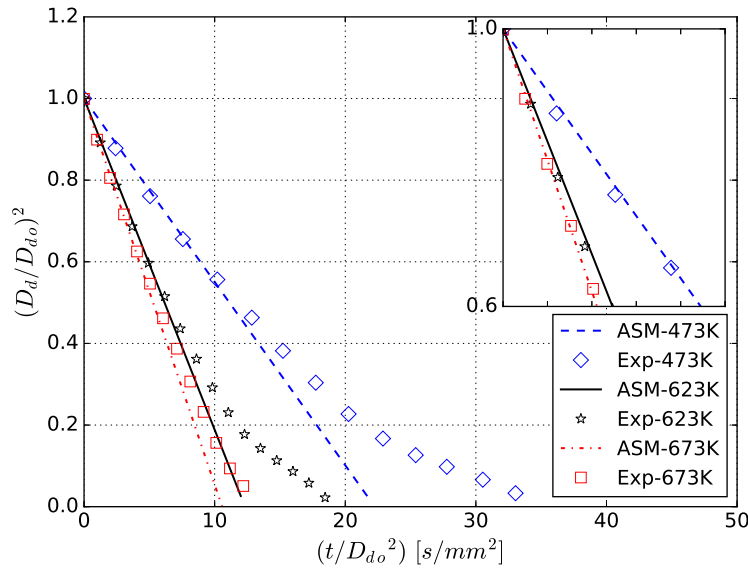
Figure 1. Normalized squared droplet diameter *versus* time for various ambient temperatures for comparison of present simulation results (lines) to the measurements (symbols).

Figure 1 shows the comparison of the normalized squared droplet diameter temporal evolution obtained of the numerical simulations and the experimental data for various ambient temperatures. This figure does not exhibit the droplet heat-up period for any ambient temperature due to limitations of the experimental procedure. As stated by Saharin *et al.* [18], since in the beginning of the experiment the droplet is transported from a cold chamber to a the furnace, they decided to show the results only when the droplet was already stabilized inside the furnace.

Moreover, it is known that after the initial heat-up period, the well-known D^2 law is obeyed, which means that the droplet surface area decreases linearly with time. As a consequence, an average area reduction rate, also known as an evaporation constant, K, can be estimated as the slope of the variation of the squared droplet diameter in the quasi-steady evaporation period. This evaporation parameter can be calculated as:

$$K = \frac{8\rho_m D_{vm}}{\rho_l}ln\left(1 + B_M\right). \tag{13}$$

The experimental data presented in Figure 1 exhibits a deviation from the linear D^2 as the droplet diameter decreases due to the interference of water vapor from the ambient gas in the anhydrous ethanol droplet evaporation,

which is caused by the hygroscopic nature of this short carbon chain alcohol [18]. In other words, as the anhydrous ethanol droplet evaporates, there is condensation of water vapor uptaken from the environment into the fuel droplet, interfering with the evaporation behavior of the anhydrous ethanol during the measurement. The impact of ambient moisture on ethanol evaporation is considered outside the scope of the present work. As shown in Figure 1, this effect gradually decreases as the ambient temperature increases and, consequently, the droplet lifetime decreases. Therefore, considering only the initial curve slope that actually represents pure ethanol evaporation, it can be concluded that the numerical results are in good agreement with the measurements for the whole range of ambient temperatures studied.
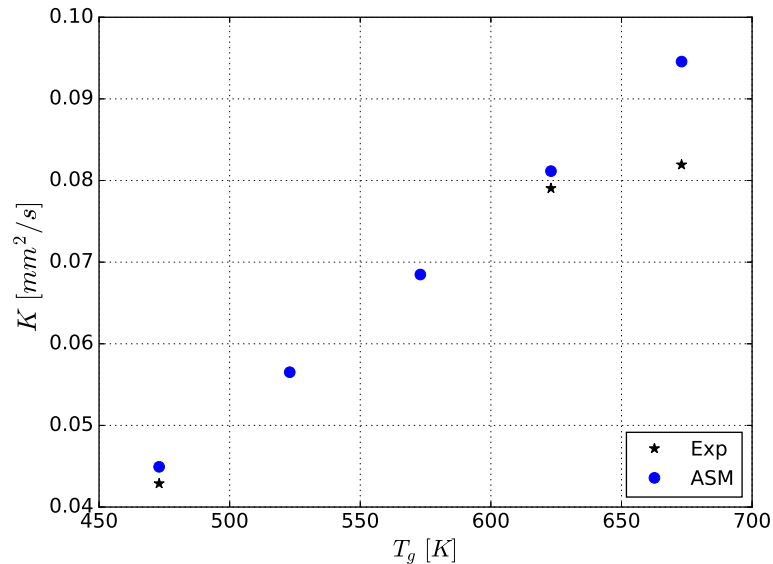
Figure 2. Experimental and numerical average area reduction rates for various ambient temperatures.

In Figure 2, the average area reduction rates for experimental and numerical results are presented. They are calculated from the data displayed in Figure 1. For 473 K, the ASM average area reduction rate is 3 % higher than the experimental one. For higher temperatures, this relative percentage difference increases. While for 623 K the ASM average area reduction rate is 5 % higher than the experimental, for 673 K it is 15 % higher.

The deviation between the ASM predictions and the experimental results might be justified by the simplifications assumed in the mathematical model, as assuming that the liquid thermal conductivity is infinitely large, which implies in no gradient temperature inside the droplet, and uncertainty factors associated to the experimental data, as the calculation error in determining the droplet diameter by analyzing images, which is of the order of 3 %; and the droplet initial temperature is not clear stated in Saharin *et al.* [18].

Effects of fuel vapor ambient concentration

In this section, the joint effect of ambient temperature and pressure together with the background fuel vapor is investigated. All the tested cases are summarized in Table **??**. The temporal variation of normalized squared droplet diameter for ambient temperature of 400 and 1000 K, ambient pressures of 0.1 and 2.0 MPa, and various ambient vapor concentrations are shown in Figure 3, while the associated temporal variation of droplet temperature are shown in Figure 4. Figures 5 and 6 present the average area reduction rates and lifetime, respectively, for all the analyzed cases. For all cases, the initial droplet diameter and temperature are 500 μm and 300 K, and the criterion suggested by Teske *et al.* [16] to determine the time step is applied for each simulation, so the time step is smaller than 10 % of the total droplet lifetime.

Table 1. Cases and computational conditions.

Cases	p_g [MPa]	T_g [K]	Y_{vg} [-]
1	0.1	400	0.0 - 0.75
2	0.1	1000	0.0 - 0.75
3	2.0	400	0.0 - 0.75
4	2.0	1000	0.0 - 0.75

When the fuel droplet is colder than the ambient gas, as in this study, the fuel vapor may condense on the droplet surface, which makes its diameter increase. It is observed, from Figure 3, that when the ambient fuel vapor mass fraction is non-zero, condensation effects are observed as an increase in the droplet diameter before its evaporation. This background fuel vapor may exist from previously evaporated droplets and its presence influences the evaporation process. Even though for the high-temperature conditions, Cases 2 and 4, the condensation effects
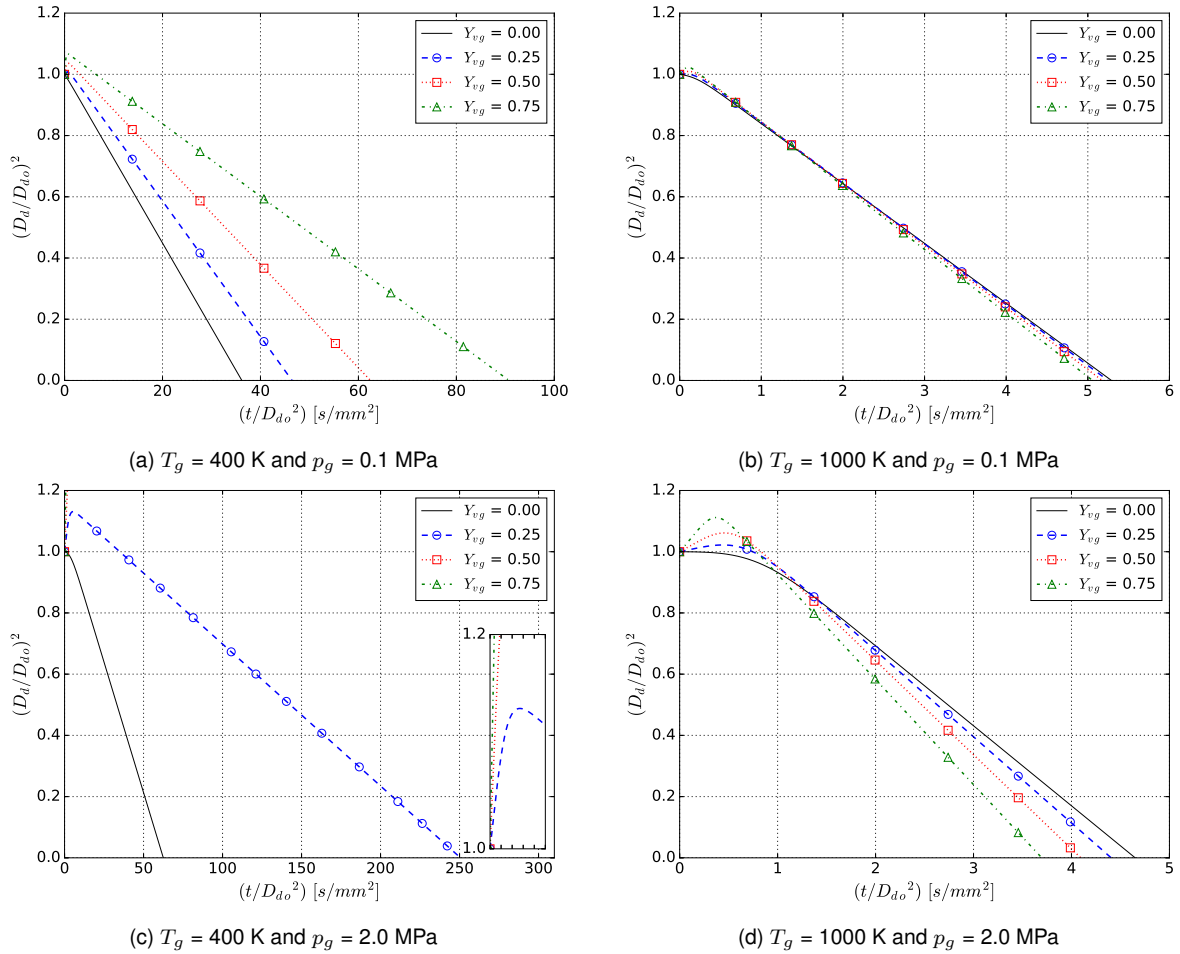
Figure 3. Normalized squared droplet diameter *versus* time for various ambient temperatures, pressures and vapor concentrations.

are attenuated, one can still detect that this effect becomes more important as the ambient fuel vapor mass fraction increases. For T_g = 400 K and p_g = 2.0 MPa, as shown in Figure 3c, the cases in which ambient fuel vapor mass fraction is equal to 0.50 and 0.75 the droplet does not evaporate, it only condensates, which is reflected by the negative average area reduction rate in Figure 5b. For this reason, the droplet lifetime observed in Case 3 is only presented in Figure6b for ambient fuel vapor mass fraction of 0.0 and 0.25.

As expected, increasing the background fuel vapor concentration causes an augmentation of the wet bulb temperature of the liquid substance, as shown in Figure 4, by the equilibrium temperature reached by the droplet after the initial heat-up period. However, the effect of the ambient fuel vapor concentration on the average area reduction rate and, consequently, on the droplet lifetime, depends on the ambient temperature, as presented in Figures 5 and 6. For the low-temperature condition, T_g = 400 K, increasing the ambient fuel vapor concentration reduces the average area reduction rate and increases the droplet lifetime. On the other hand, for the high-temperature condition, T_g = 1000 K, increasing the ambient fuel vapor concentration increases the average area reduction rate and reduces the droplet lifetime, and this effect is still accentuated for higher ambient pressure, as in Cases 3 and 4. For T_g = 1000 K and p_g = 0.1 MPa, an increase of the ambient fuel vapor concentration from 0.0 to 0.75 leads to an increase of 6 % in the average area reduction rate and a decrease of 4 % in the droplet lifetime. Meanwhile, for T_g = 1000 K and p_g = 2.0 MPa, there is an increase of 31 % in the average area reduction rate and a decrease of 21 % in the droplet lifetime.

Investigations based on results presented in this section reveal that there is also a threshold ambient gas temperature that determines whether the average area reduction rate will increase or decrease as the ambient vapor concentration is enhanced. This behavior can be explained by the existence of two competing factors that influence the evaporation behavior: mass and energy transfer. Firstly, increasing the ambient vapor concentration reduces the mass transfer, more specifically due to mass diffusion reduction, which is expressed as a decrease in the Spalding mass transfer number (Eq. 5) and, consequently, a reduction in the average area reduction rate. Secondly, increasing the ambient vapor concentration might enhance the energy transfer rate depending on the ambient temperature, increasing the Spalding energy transfer number (Eq. 10) and, as a result, the average area reduction rate is also increased.

For T_g = 400 K, as studied in Cases 1 and 3, both the Spalding mass and energy transfer numbers decrease as the ambient fuel vapor concentration increases. Thus, both terms from Eq. (13) decrease, causing the average area reduction rate to reduce for low-temperature conditions. Meanwhile, for T_g = 1000 K, as studied in Cases 2 and 4,
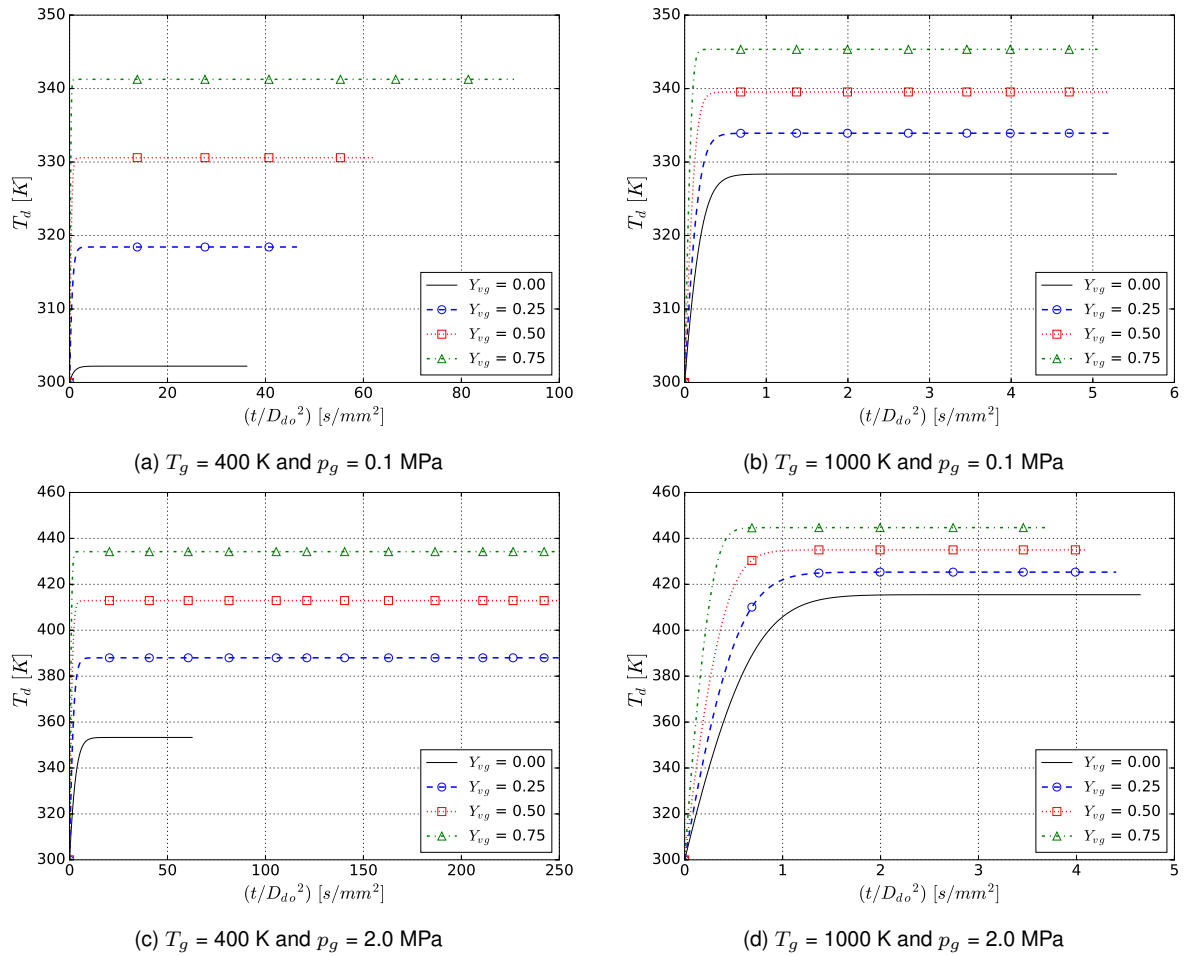
Figure 4. Droplet temperature *versus* time for various ambient temperatures, pressures and vapor concentrations.
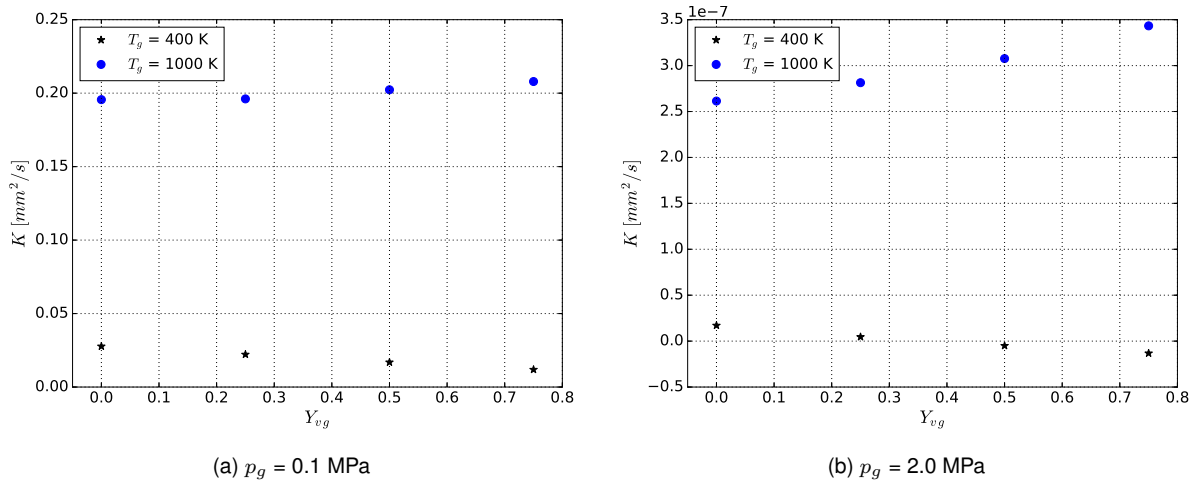
Figure 5. Average area reduction rates for various ambient temperatures, pressures and vapor concentrations.

the Spalding mass transfer number continues to decrease as the ambient fuel vapor concentration increases, but the Spalding energy transfer number increases. For p_g = 0.1 MPa, an ambient fuel vapor concentration increase from 0.0 to 0.75 leads to a decrease of 26 % in Spalding mass transfer number and an increase of 2 % in the Spalding energy transfer number, and there is a decrease of 9 % in Spalding mass transfer number and an increase of 8 % in the Spalding energy transfer number for p_g = 2.0 MPa. If the two terms from Eq. (13), $\rho_m D_{vm}/\rho_l$ and $ln\left(1 + B_M\right)$, are examined, for p_g = 0.1 MPa, an increase of 33 % in the first term and a decrease of 20 % in the second term is observed, resulting in an increase of 6 % in the average area reduction rate previously cited. For p_g = 2.0 MPa, the first term increases with 41 % and the second reduces with 7%, which increases the average area reduction rate of 31%.

Hence, how the average area reduction rate is influenced by the ambient vapor concentration is determined by the

(a) p_g = 0.1 MPa

(b) p_g = 2.0 MPa
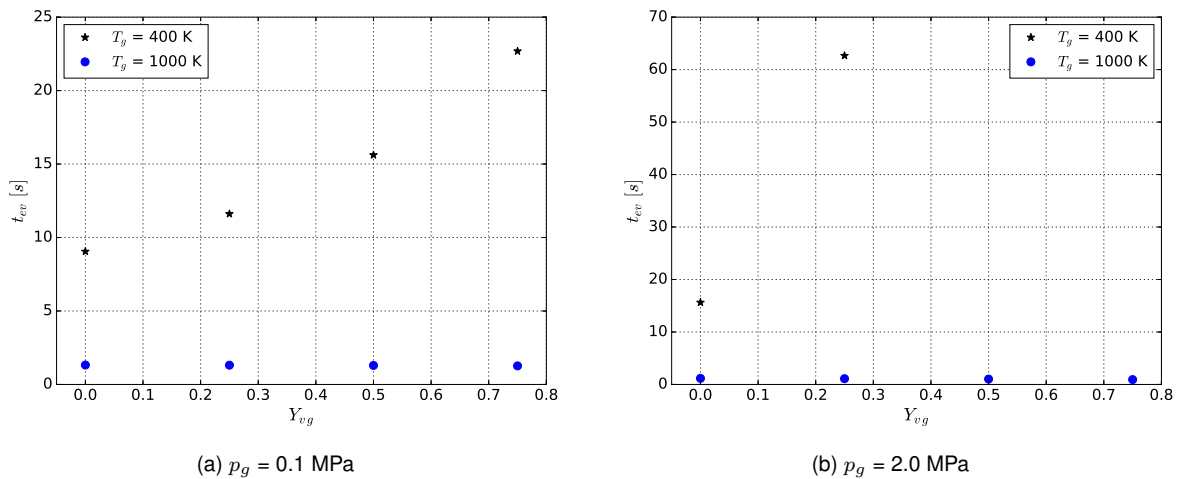
Figure 6. Droplet lifetime for various ambient temperatures, pressures and vapor concentrations.

net result of those two factors, namely, the mass transfer and energy transfer factors. For ambient temperatures below the threshold temperature, the first factor predominates. However, when the ambient temperature is higher than the threshold temperature, the second factor has a stronger impact on the average area reduction rate than the first. As can be observed from Figure 5, the first factor predominates for ambient temperature of 400 K, since the average area reduction rate decreases as the ambient vapor concentration increases. However, for T_g = 1000 K the behavior is the opposite.

Unitary Lewis number, Le = 1, is a widely used assumption in the analysis of droplet evaporation and/or combustion [15]. When theoretical models are derived based on this assumption, they consider that mass diffusivity and thermal diffusivity are equal. Even though this is usually a good assumption for high-temperature and dilute cases and in the absence of background fuel vapor, it is important to highlight that for the cases considered in this study, where the ambient fuel vapor mass fraction is 0.75, the Lewis number computed throughout the simulations tends to approximately 0.6. Therefore, for problems involving multiple droplets evaporation, specially in dense condition, assuming a Lewis number of unity may not be accurate.

Conclusions

The influence of gas ambient conditions, including pressure, temperature and vapor concentration, on the evaporation behavior of a single ethanol droplet is thoroughly investigated in this study. The impact of the background fuel vapor concentration on the evaporation of a single droplet is examined in the range of $0.0-0.75$ for ambient pressure and temperature varying between $0.1-2.0$ MPa and $400-1000$ K, respectively. Condensation effects are observed in the beginning of the simulation, and, once the droplet temperature increases, the droplet starts to evaporate, which is confirmed by its reduction. Nevertheless, in some cases, such as for T_g = 400 K and p_g = 2.0 MPa, if the ambient vapor concentration is higher than 0.25, the droplet does not evaporate. As a matter of fact, its diameter only increases as a function of time. Furthermore, it is also noticed that the effect of the background fuel vapor concentration on the average area reduction rate depends on the ambient temperature, similar to the effect of ambient pressure, as previously stated. For T_g = 400 K the average area reduction rate decreases as the ambient vapor concentration increases, while for T_g = 1000 K the behavior is the opposite.

The findings achieved in the model validation are in good agreement with previous researches available in the literature [19]. In the background fuel vapor concentration effects analysis, for cases of low ambient temperature and low ambiente pressure, the findings of Abarham and Wichman [2] for propane evaporation follows the same trend as observed in this work for ethanol evaporation. If both low and high conditions are investigated, it can be seen that the effect of background fuel vapor concentration on the average area reduction rate depends on the ambient temperature. Moreover, for the specific condition of low ambient temperature and high ambient pressure, it is concluded that if the background fuel vapor concentration is high enough, the droplet does not evaporate.

Acknowledgements

Nomenclature

μ	dynamic viscosity [kg/(m s)]
ρ	density [kg/m^3]
χ_v	vapor molar fraction [-]
B_M	Spalding mass transfer number [-]
B_T	Spalding energy transfer number [-]

c_p	specific heat capacity [J/(kg K)]
D_d	droplet diameter [m]
D_v	vapor diffusion coefficient [m^2/s]
K	average area reduction rate [m^2/s]
k	thermal conductivity [J/(m s K)]
Le	Lewis number [-]
L_v	specific latent heat of evaporation [J/kg]
m_d	droplet mass [kg]
$\dot{m}_d$	droplet mass evaporation rate [kg/s]
Nu	Nusselt number [-]
p	pressure [Pa]
Q_S	sensible energy per unit of time [J/s]
Sh	Sherwood number [-]
T_d	droplet temperature [K]
Y_v	vapor mass fraction [-]

References

[1] (2016). International Energy Outlook, https://www.eia.gov/outlooks/ieo/pdf/0484(2016).pdf

[2] Abarham, M. and Wichman, I. S. (2011). Mono-component fuel droplet evaporation in the presence of background fuel vapor. *International Journal of Heat and Mass Transfer*, 54(17):4090–4098.

[3] Abramzon, B. and Sirignano, W. (1989). Droplet vaporization model for spray combustion calculations. *International Journal of Heat and Mass Transfer*, 32(9):1605–1618.

[4] Agarwal, A. K. (2007). Biofuels (alcohols and biodiesel) applications as fuels for internal combustion engines. *Progress in Energy and Combustion Science*, 33(3):233–271.

[5] Bergthorson, J. M. and Thomson, M. J. (2015). A review of the combustion and emissions properties of advanced transportation biofuels and their impact on existing and future engines. *Renewable &D Sustainable Energy Reviews*, 42(Supplement C):1393–1417.

[6] Ghassemi, H., Baek, S. W., and Khan, Q. S. (2006). Experimental study on binary droplet evaporation at elevated pressures and temperatures. *Combustion Science and Technology*, 178(6):1031–1053.

[7] Goodwin, D. G., Moffat, H. K., and Speth, R. L. (2016). Cantera: An object-oriented software toolkit for chemical kinetics, thermodynamics, and transport processes. http://www.cantera.org. Version 2.2.1.

[8] Green, D. W. and Perry, R. H. (2007). *Perry's Chemical Engineers' Handbook*. McGraw-Hill, New York, USA, 8 edition.

[9] Harstad, K. and Bellan, J. (2000). An all-pressure fluid drop model applied to a binary mixture: heptane in nitrogen. *International Journal of Multiphase Flow*, 26(10):1675–1706.

[10] Kitano, T., Nishio, J., Kurose, R., and Komori, S. (2014). Effects of ambient pressure, gas temperature and combustion reaction on droplet evaporation. *Combustion and Flame*, 161(2):551–564.

[11] Ma, L., Naud, B., and Roekaerts, D. (2016). Transported PDF modeling of ethanol spray in hot-diluted coflow flame. *Flow, Turbulence and Combustion*, 96(2):469–502.

[12] Nomura, H., Ujiie, Y., Rath, H. J., Sato, J., and Kono, M. (1996). Experimental study on high-pressure droplet evaporation using microgravity conditions. *Symposium International on Combustion*, 26(1):1267–1273.

[13] Pinheiro, A. P. and Vedovoto, J. M. (2018). Evaluation of droplet evaporation models and the incorporation of natural convection effects. *Flow, Turbulence and Combustion*.

[14] Quiroga, L. C. R., Balestieri, J. A. P., and Ávila, I. (2017). Thermal behavior and kinetics assessment of ethanol/gasoline blends during combustion by thermogravimetric analysis. *Applied Thermal Engineering*, 115(Supplement C):99–110.

[15] Sazhin, S. S. (2006). Advanced models of fuel droplet heating and evaporation. *Progress in Energy and Combustion Science*, 32(2):162–214.

[16] Teske, M. E., Thistle, H. W., and Londergan, R. J. (2009). Considerations of time step and evolving droplet size in the simulation of fine droplet motion using AGDISP. In *Proc. of 2009 ASABE Annual International Meeting*. ASABE.

[17] Westbrook, C. K. (2013). Biofuels combustion. *Annual Review of Physical Chemistry*, 64(1):201–219.

[18] S. B. Saharin, B. Lefort, C. Morin, C. Chauveau, L. L. Moyne, R. Kafafy, Vaporization characteristics of ethanol and 1-propanol droplets at high temperatures, Atomization and Spray 22 (3) (2012) 207–226.

[19] M. Al Qubeissi, N. Al-Esawi, S. S. Sazhin, M. Ghaleeh, Ethanol/gasoline droplet heating and evaporation: Effects of fuel blends and ambient conditions, Energy & Fuels 32 (6) (2018) 6498–6506.